文章编号：0258-8013 (2008) 11-0087-07　　中图分类号：TM 615; TK 514　　文献标识码：A　　学科分类号：470·40

抛物槽式太阳能热发电系统的模拟分析

曲　航[1]，赵　军[1]，于　晓[2]

(1. 天津大学机械工程学院，天津市 南开区 300072；2. 鲁东大学土木工程学院，山东省 烟台市 264025)

Simulation of Parabolic Trough Solar Power Generating System for Typical Chinese Sites

QU Hang[1], ZHAO Jun[1], YU Xiao[2]

(1. School of Mechanical Engineering, Tianjin University, Nankai District, Tianjin 300072, China;
2. School of Civil Engineering, Ludong University, Yantai 264025, Shandong Province, China)

ABSTRACT: Parabolic trough concentrating solar power (CSP) has great potential in China, and it is necessary to study the operation performance of the CSP plant located in typical sites of China, for reference of the feasibility study of this technology in China. A parabolic trough CSP plant of 35 MW was simulated with Solar Thermal Electric Components(STEC) model in the environment of TRNSYS (version 16) for nine sites in three typical Chinese regions, respectively. The system model was established according to Rankine principle. The simulation results indicate that Tibet and Xinjiang are more suitable for locating the CSP plant due to their high direct normal insolation(DNI). The annual electricity output of the Lhasa project is 101.6% higher than that of Naiman. As a critical factor to evaluate the system performance, the annual solar-electricity efficiency in the range of 9%~14%, can be realized with the simulated 35 MW plants in 9 selected sites. Also the influence of solar field size to the system performance was studied, and the result reveals that the optimal field size shifts to a higher value with decreasing DNI.

KEY WORDS: concentrating solar power; parabolic trough; direct normal insolation; site selection; feasibility study

摘要：抛物槽聚焦式太阳能发电有着广阔的发展前景，有必要通过系统仿真的方法对其在中国典型地区的运行性能进行分析，以便为该项技术在中国的可行性研究提供参照。运用STEC模块在TRNSYS环境下，按照朗肯循环原理建立 35 MW槽式电站的仿真模型，在中国 3 个典型地区：西藏、新疆和内蒙古，选取 9 个地点对电站运行进行模拟。模拟结果表明，由于全年直射辐射强度较高，西藏和新疆地区更适合于建设该类电站，拉萨电站年发电量相对于位于内蒙古奈曼旗的电站要高出 101.6%；作为衡量聚焦式太阳能电站系统性能的重要参数，电站的年光电转化效率可达 9%~14%。同时提出了最佳集热器阵列面积的概念，模拟计算表明，该最佳面积随着直射太阳辐射通量的降低逐渐增大。

关键词：聚焦式太阳能发电；抛物槽；直射辐射强度；选址；可行性研究

0 INTRODUCTION

Due to rapid expansion of energy-intensive industry sectors, the annual electricity demand in China had been growing at an average of 14.6% from 2002 to 2005. China has to build more and more power plants, and this trend is expected to exist further in the near and mid term[1].

Coal is the major energy resource for power generation in China, representing 75.9% in total in 2005[2]. Environmental negative influences caused by the dominant use of coal for electricity generation, such as ash disposal, air pollution and climate change, have been felt by Chinese people.

Chinese government is looking for environment friendly renewable energy sources for electricity generation. Concentrating solar power(CSP) is a solution for pollution reduction, whose principle is similar to that of a conventional power plant, while the thermal energy driving Rankine steam power cycle is transferred from fuel combustion to solar radiation.

CSP system includes three different design alternatives: parabolic trough, tower and dish [3-5]. Parabolic trough technology has been demonstrated mature by the nine solar power plants developed by Luz International Inc. from 1984 to 1990. The

基金项目：国家“十一五”科技支撑计划项目(2006BAA01B04)。
The National Key Technologies R&D Program in the 11th Five-year Period of China(2006BAA01B04).

up-to-22 years' operation experiences of these plants indicate a low technical and financial risk in developing near-term projects [6-8]; in the field of scientific research, 64% of funding had been granted to develop parabolic technology, while 31% for dish/stirling and solar tower together. This indicates that further large commercialization of parabolic technology will be realized in the near or mid term [9].

However, compared with some developed countries, such as America, Australia and Germany, the research in the field of CSP is still at the preliminary stage in China.

1 SITE SELECTION

1.1 ESTABLISHMENT OF MODELS

It is the core of the feasibility study of CSP to identify suitable sites for a plant. There are many siting factors related to technical, environmental and economic perspectives. Most of these factors are same to those of a fuel-fired plant. The differences lie in site topography, land area required for the solar field, the nature of the heat transfer fluid that flows through the solar field to collect heat, and the positive environmental effects, such as less emissions due to reduction use of fossil fuel[10].

The most crucial siting factor for a CSP plant is abundant solar resource. It is generally assumed that CSP are only economical for locations with direct incidence radiation above 1 800 kWh/(m^2·a)[11]. Secondly, site topography is another important factor. An overall slope of less than 1% is preferable; higher slope up to 3% is also acceptable, but the cost will be higher[10]. Thirdly, a large area of land with low density of population is preferred to locate the huge solar field of a CSP plant.

China is the third largest country in the world, with variable conditions all around the country. Tibet Autonomous Region, Inner Mongolia Autonomous Region and Xinjiang Autonomous Region are best candidates according to the above mentioned requirements.

In this study, the following 9 sites were selected as the candidates: ① Lhasa(Latitude(Lat.) 29.43ºN, longitude(Long.) 91.02ºE), Xigaze(Lat. 29.15ºN, Long. 88.53ºE) and Qamdo(Lat. 31.09ºN, Long. 97.10ºE), representing Tibet region; ②Hohhot(Lat. 40.78ºN, Long. 111.62ºE), Linhe(Lat. 40.83ºN, Long. 107.50ºE) and Naiman(Lat. 43.28ºN, Long. 121.30ºE), representing the Inner Mongolia region; ③Urumqi (Lat. 43.8ºN, Long. 87.58ºE), Hami(Lat. 42.8ºN, Long 93.45ºE) and Kashi(Lat. 39.48ºN, Long. 75.97ºE), representing the Xinjiang region.

These districts have diverse meteorological conditions, which affect the performances of CSP plants greatly.

To study the effect of direct solar radiation on the power output and the efficiency of the solar power generation in the selected sites, both ambient temperature and DNI are taken as input of the performance simulation and analysis of the solar field and the associated power block.

Fig.1 shows the schematic of the process flow of a parabolic solar thermal power plant, in which the principle of Rankine is followed.

There is recognized scale-up cost reduction for the parabolic thermal power plant[12]. In the present research, a power plant of 35 MW was simulated in the TRNSYS (Version 16) environment and the model library STEC[13-14].

The simulated plant has an identical process flow to the traditional one except for the component of solar field. The solar field consists of arrays solar collector assemblies (SCA). The LS-2 generation collector is used in SCA, whose parameters are listed in Tab.1[15].

表 1 槽型抛物面太阳能集热器组件的主要参数

Tab. 1 Main parameters of the parabolic trough solar collector assemblies

Collector type	Collector length/m	Aperture width of SCA/m	Aperture area of single solar collector /m^2
LS-2	47.1	5.0	235
Focal length of SCA/m	Inner diameter of the absorber/m		Outer diameter of the absorber/m
1.49	0.065 5		0.070

Besides the solar field, the other components all belong to the power cycle. The steam generation system consists of a single-phase economizer, an evaporator and a superheater. The overall heat transfer coefficient UA is scaled with the cold side mass flow rate according to power law; the components of preheater and subcooler together model the feed water heater, where the feed water is heated by the steam

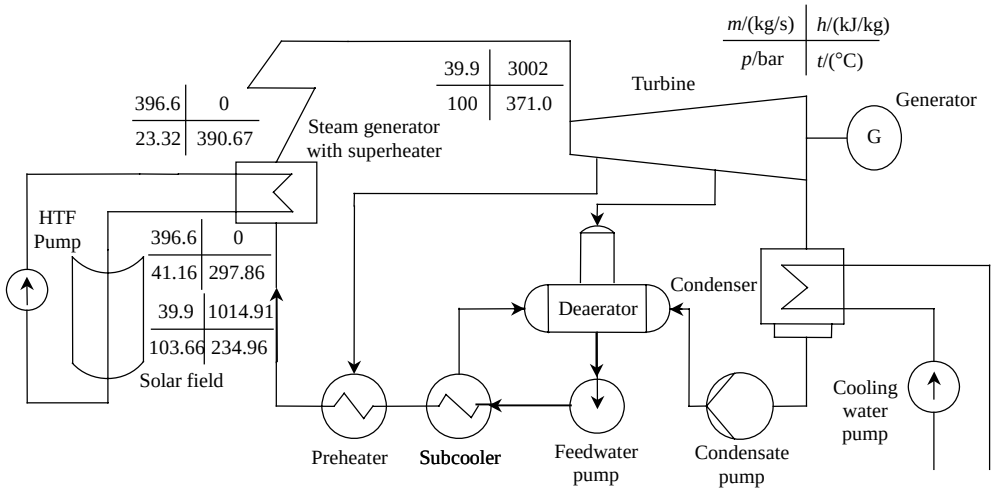

图 1　太阳能电站系统图

Fig. 1　Overview of the solar power plant with Rankine Process

from turbine before it flows to the economizer; in the deareator the oxygen is purged from the feed water, where the steam from turbine extraction is mixed with condensate driven by the condensate pump; the condenser condenses the steam exiting from turbine and discharges the heat through cooling tower, so that the condensate can be further pumped to steam generation system. The turbine of the simulated plant has extractions, where the steam is derived to heat the preheater and the deaerator.

Tab.2 shows the simulation conditions for the CSP plant, including DNI at design point, collector outlet temperature and optical efficiency of the collector, etc..

表 2　电站仿真的相关参数

Tab. 2　Simulation conditions of the CSP plant

Condition	Value
Direct normal insolation at the design point/(W/m^2)	800
Demanded outlet temperature/℃	390
Concentration ratio	71
Mirror reflectivity	0.94
Mirror transmission	0.98
Quality factor of the mirror	0.88
Glass envelope transmission	0.96
Absorber tube absorptivity	0.96

The STEC parabolic trough collector is based on the model of Lippke[16], using an integrated efficiency equation to account for different fluid temperatures at the field inlet and outlet of the collector field. It calculates the demanded mass flow rate of the heat transfer fluid to achieve a user-defined outlet temperature T_{out} by

$$\dot{M}=\frac{\dot{Q}_a-\dot{Q}_l}{C_p(T_{out}-T_{in})} \tag{1}$$

Where $\dot{M}$ is the mass flow rate of the heat transfer fluid, kg/hr; $\dot{Q}_a$ and $\dot{Q}_l$ are the absorbed heat and heat loss of the piping respectively, kJ/hr; C_p is the specific heat of the heat transfer fluid, kJ/(kg·℃); T_{in} and T_{out} are the inlet and demanded outlet temperature of the solar field respectively.

The absorbed heat is calculated by

$$\dot{Q}_{abs}=A_a I_b(\cos\theta)\eta \tag{2}$$

In which A_a is the solar field area, m^2; I_b is the DNI, kJ/(h·m^2); θ is the incident angle; the absorber efficiency η is calculated by

$$\eta=K\times M\times N\times[A+B\times\frac{\Delta T_{in}+\Delta T_{out}}{2}]+(C+D\times w)\times\frac{\Delta T_{in}+\Delta T_{out}}{2\times I_b}+E\times\frac{\Delta T_{in}\times\Delta T_{out}+(\Delta T_{out}-\Delta T_{in})^2/3}{I_b} \tag{3}$$

In which the coefficients *A*, *B*, *C*, *D* and *E* are empirical factors describing the performance of the collector, and they were specified by Dudley etc. for SEGS LS-2 collector[15-16]; factor *K* is the incident angle modifier; *M* is the factor considering end losses, and *N* is the factor considering shading of parallel rows. These 3 factors were evaluated by Lippke[14]; ΔT_{in} and ΔT_{out} are the differences between the collector inlet and outlet temperature and the ambient temperature, respectively, ℃; *w* is the wind speed, m/s.

$\dot{Q}_l$ accounts for piping heat losses by empirical coefficients and can be calculated by

$$\dot{Q}_l = 72A_a(T_{mean} - T_{amb})/343 \quad (4)$$

In which T_{amb} is the ambient temperature, ℃; 72 kJ/(h·m^2) and 343℃ are reference values for heat loss and temperature difference, respectively; T_{mean} is the mean temperature of the solar field, ℃, and it is calculated as

$$T_{mean} = (T_{in} + T_{out})/2 \quad (5)$$

1.2 VALIDATION OF MODELS

To validate the established model, the calculated mass flow rate is compared with the measured results of Californian Solar Electric Generation Station (SEGS Ⅵ)[17] of a clear day in May in 2005(Fig.2). The prediction is upon the scenario of a constant solar field outlet temperature of 390℃. The figure shows that the mass flux q_m calculated from the established model agrees well with the measured plant data, with deviation usually less than 10%. The variation at the time of start up is due to the operation strategy of quickly commissioning the turbine, and that at the time of shutdown is due to the pant operating procedure during which a minimum flow rate of 1 440 000 kg/h[17] is always maintained. The comparison indicates that the model can be applied to simulate the most important process of a designed collector field.

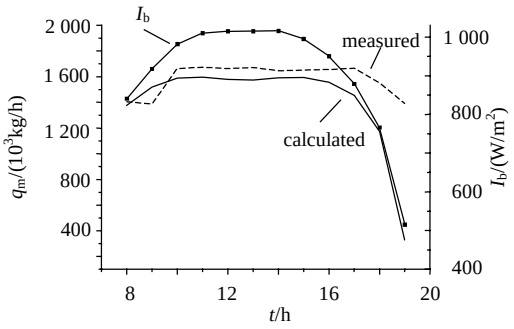

图 2 SEGS Ⅵ电站的流量模拟值和实测值的对比

Fig. 2 Comparison of the calculated and measured mass flow rate for SEGS Ⅵ plant

2 SIMULATION RESULTS AND DISCUSSIONS

2.1 ELECTRICITY OUTPUT FOR THE SIMULATED PLANTS

The nine 35MW-projects in the 3 autonomous regions were simulated respectively and the performances for various sites were studied. The 'Meteonorm' weather files distributed with TRNSYS software and the 'EnergyPlus' weather data were used as inputs for the simulation[18-19].

TRNSYS model of the Integrator (type 24) was applied to calculate the annual electricity output W_a of the nine simulated plants(Fig.3). It can be seen that the electricity output is approximately proportional to DNI, this indicates that the annual DNI level is the most important parameter for plant generation capability. The study on the angle of a countrywide siting shows that Tibet and Xinjiang should be highlighted for all the 4 best electricity producers located in these 2 regions.

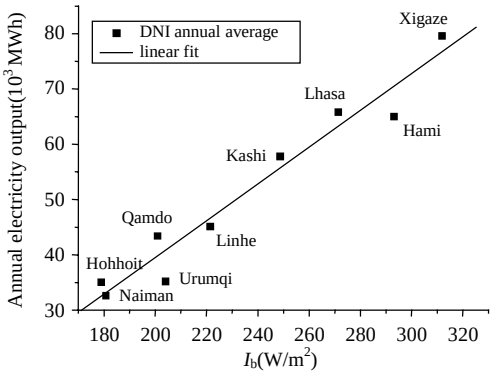

图 3 各地电站的年发电量与直射辐射通量的关系

Fig. 3 Annual electricity generation in dependence on DNI for the selected 9 sites

Fig.4 and Fig.5 show the monthly electricity output W_m of the projects in Lhasa and Naiman(which is located in the east of Inner Mongolia). Basically it is indicated in the figures that the monthly power outputs of the plants increase with the radiation level. However, exceptions exist in several months for both projects, and this can be explained by the influence of the ambient temperature (Tab.3).

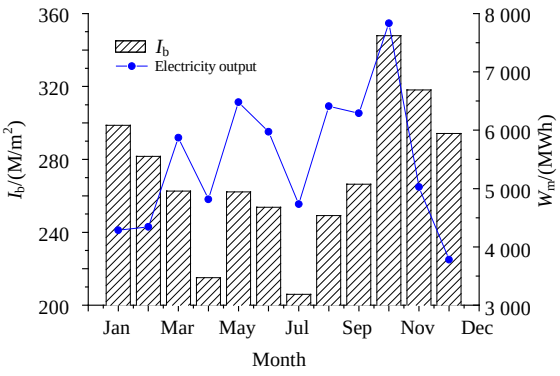

图 4 拉萨电站的逐月发电量

Fig. 4 Monthly electricity output for the Lhasa project

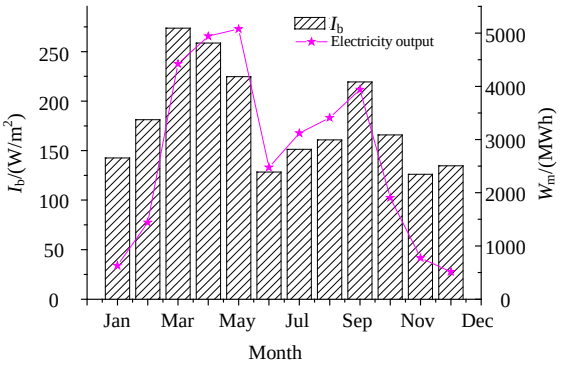

图 5　奈曼旗电站的逐月发电量

Fig. 5　Monthly electricity output for the Naiman project

表 3　拉萨和奈曼旗两地的月度气象数据

Tab. 3　Monthly weather data for Lhasa and Naiman

Month	Ambient temperature/℃		Wind speed/(m/s)	
	Lhasa	Naiman	Lhasa	Naiman
January	−5.8	−14.8	1.9	3.7
February	−2.7	−11.3	2.3	3.8
March	1.2	−2.8	2.3	4.5
April	4.4	7.3	2.3	5.0
May	8.5	15.1	2.1	4.6
June	11.9	19.6	2.0	3.7
July	11.9	22.5	1.7	3.4
August	11.2	21.0	1.5	2.9
September	9.4	14.1	1.5	3.4
October	4.5	6.7	1.5	3.9
November	−1.7	−4.2	1.4	3.7
December	−5.4	−11.7	1.5	3.4

With an annual output of 65 843.3 MWh, Lhasa project is 101.6% more productive than Naiman project(annual power 32 652.5 MWh). Obviously it is contributed by the much higher DNI level(annual) in Lhasa(Fig.3). Due to the similar reason, the electricity output difference between the two projects is even larger in winter, and this is especially important to plant siting if the load curve is considered.

2.2　DISCUSSION OF SYSTEM EFFICIENCY

The system efficiency is a crucial parameter to evaluate the performance of a CSP plant, and it is defined as the ratio of the electrical power produced by the cycle to the thermal energy supplied to the cycle

$$\eta_{\text{system}} = \frac{W_{\text{electric}}}{I_{\text{incident}} A_{\text{a}}} \tag{6}$$

Where η_{system} is the system efficiency; W_{electric} is the electrical power output, W; I_{incident} is the incident solar radiation, W/m^2.

The incident solar radiation I_{incident} in eq.(6) is determined by eq.(7)

$$I_{\text{incident}} = KI_{\text{b}} \cos\theta \tag{7}$$

Fig.6 and Fig.7 show the influences of the annual average meteorological data on DNI, ambient temperature T_{a} and wind speed w, on the annual system efficiency. The figures show that the system efficiency of various projects ranges from 9% to 14%.

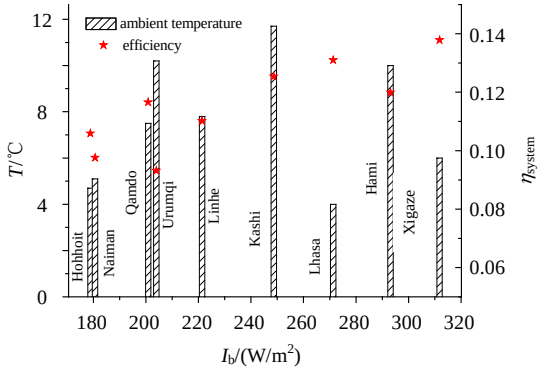

图 6　各地电站系统效率与直射辐射通量及环境温度的关系

Fig. 6　System efficiency in dependence on DNI and influence of ambient temperature for selected 9 sites

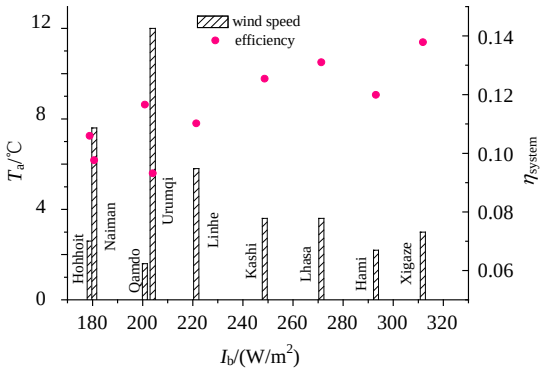

图 7　各地电站系统效率与直射辐射通量及风速的关系

Fig. 7　System efficiency in dependence on DNI and influence of wind speed for selected 9 sites

Generally the system efficiency increases with increasing DNI, increasing ambient temperature and decreasing wind speed, but the increase is not obvious. The overall system efficiency is a product of solar field efficiency and power cycle efficiency. The solar field efficiency decreases with the increase of outlet temperature, while an opposite trend is seen in the power cycle. So the change of system efficiency against outlet temperature is small. Therefore, operation at a wide range of solar field temperature and flow rate, which is the result of the change of the meteorological data, produce no discernible difference in system efficiency.

3 SIZE OF SOLAR FIELD

The cost of solar field accounts for over 50% in the total investment of the plant[20], so it is very important to determine an optimum field size in the plant design, especially a solar-only plant.

In this section, a field size study on three projects of Naiman, Linhe and Lhasa, whose annual DNI levels are 1 582, 1 939 and 2 376 kWh/(m^2a), respectively, is performed. The annual ambient temperature of these 3 sites are 5.1 ℃, 10.2 ℃, and 4 ℃, while the annual wind speed are 3.8 m/s, 6 m/s and 1.8 m/s, respectively. Fig.8 shows the annual electricity generation and efficiency at different annual DNI levels for 35 MW solar trough power plants with various solar field sizes.

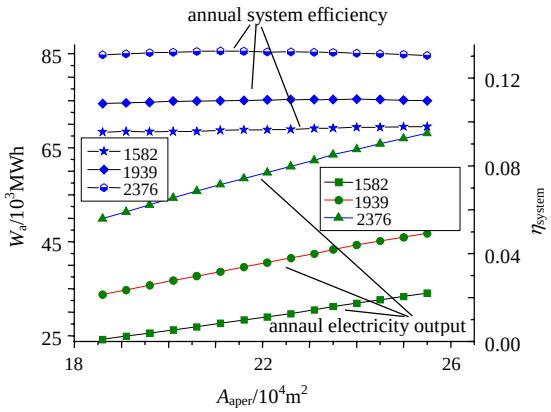

图 8 不同全年直射辐射通量下太阳能阵列面积与全年发电量及系统效率的关系

Fig. 8 Annual electricity generation and efficiency in dependence on solar field size for different irradiation

The simulation results in the above 3 meteorological conditions show the same characteristics. The annual electricity increases almost linearly with the increase of solar field size. However, it is shown in figure that the most efficient solar field size drifts to higher values with the decrease of irradiance. An inflexion exists for every curve of the system efficiency, the critical point in the project of Naiman, Linhe and Lhasa is 255 000 m^2, 240 000 m^2 and 211 000 m^2, respectively.

4 CONCLUSIONS

Utilizing solar energy as source, the parabolic trough concentrating solar power (CSP) technology has potential to become part of the solutions for current energy and environment problems in China.

In this paper, the STEC model was applied to establish a 35MW plant model in the TRNSYS (version 16.0) environment. The performances of plants in Tibet, Inner Mongolia and Xinjiang were studied respectively and the following results were revealed:

（1）If the angle of solar radiation is considered, Tibet and Xinjiang should be highlighted in the 3 regions for siting CSP plant. Lhasa project is 101.6% more productive than Naiman project due to its much higher DNI level.

（2）An annual solar-to-electricity efficiency in the range of 9-14% can be reached for the simulated 35 MW plant.

（3）The influence of solar field area to the system performance was also studied, and it is found that with the decrease of DNI the optimal field size shift to a higher value.

However, other siting factors including site topography, land use and transmission availability must be investigated before a plant site is determined.

REFERENCES

[1] Kahrl F，Roland-Holst D．China’s carbon challenge：insights from the electric power sector[R]．Berkeley，California，2006．

[2] 张绍强，张运章．我国煤炭资源、生产与环境概况[J]．环境保护，2006，(13)：53-57．
Zhang Shaoqiang，Zhang Yunzhang. Resources，production and environmental issues of coal in China[J]．Environmental Protection，2006，(13)：53-57(in Chinese)．

[3] Theocharis T，Vasilis G，Katerina M．Technical and economical evaluation of solar thermal power generation[J]．Renewable Energy，2003，28 (6)：873-886．

[4] Cohen G，Kearney D W，Cable R G．Recent improvements and performance experience at the Kramer Junction SEGS Plants [C]．Proceedings of the Solar 1996，San Antonio，TX，1996．

[5] Tyner C，Kolb G J，Meinecke W，et al．Concentrating solar power in 1999[R]．Paris，1998．

[6] Price H．Executive summary：assessment of parabolic trough and power tower solar technology cost and performance forecasts [R]. NREL/SR-550-35060. Sargent & Lundy LLC Consulting Group，Chicago，Illinois，2003．

[7] Mills D．Advances in solar thermal electricity technology[J]．Solar Energy，2004，76 (1-3)：19-31．

[8] Hank Price．Parabolic trough solar thermal electric power plants [R]. DOE/GO-102003-1740，National Renewable Energy Laboratory，Golden，Colorado，2003．

[9] Kfw Bankengrup. Hochtemperatur solarthermische Stromerzeugung [R]. Frankfurt，Germany，2004.

[10] Gilbert Cohen，Mark Skowronski，Robert Cable，et al. Solar thermal parabolic trough electric power plants for electric utilities in California[R]. Solargenix Energy. Raleigh，NC，the United State of America，2005.

[11] Hans M，Franz T. Concentrating solar power-a review of the technology[J]. Ingenia，2004，(18)：43-50.

[12] Sargent & Lundy LLC Consulting Group. Assessment of parabolic trough and power tower solar technology cost and performance forecasts[R]. Chicago，Illinois，2003.

[13] Klein S A，Beckman W A，Duffie J A，et al. TRNSYS：a transient system simulation program[R]. Madison：Solar Energy Laboratory，University of Wisconsin，Madison，WI，the United States，2006.

[14] Peter Schwarzbözl. A TRNSYS model Libiary for solar thermal electric components(STEC)[R]. Köln，Germany，2006.

[15] Dudley V，Kolb G，Kearney D. SEGS LS-2 solar collector：test results [R]. Albuquerque，NM，the United States，1994.

[16] Dudley V，Evans L R，Matthews C W. Test results industrial solar technology parabolic trough solar collector[R]. Albuquerque，NM，the United States，1995.

[17] Lippke F. Simulation of the part-load behavior of a 30 MWe SEGS plant[R]. Albuquerque，New Mexico，the United States，1995.

[18] Meteotest. Meteonorm Handbook[R/OL]. Bern，Switzerland. Oct，2007. http://www.meteonorm.com/pages/de/downloads.php.

[19] U. S. Dept. of Energy. EnergyPlus Handbook[R/OL]. Washington DC， USA. Oct， 2007. http://www.eere.energy.gov/buildings/energyplus/
cfm/weather_data.cfm.

[20] Pilkington Solar International GmbH. Statusbericht Solarthermische Kraftwerke[R]. Köln，Germany，1996.

收稿日期：2007-08-28。

作者简介：

曲　航(1969—)，男，博士研究生，主要从事太阳能集热蓄热技术及太阳能热发电电站系统仿真的研究，quhang0922@yahoo.com.cn；

赵　军(1964—)，男，教授，主要从事太阳能、浅层地热能等可再生能源的利用研究，zhaojun@tju.edu.cn。

(编辑　刘浩芳)